catalysts

MDPI

Article

Efficient Oxidative Dehydrogenation of Ethylbenzene over K/CeO_2 with Exceptional Styrene Yield

He Sun, Juping Zhang, Kongzhai Li, Hua Wang and Xing Zhu *

State Key Laboratory of Complex Nonferrous Metal Resources Clean Utilization, Faculty of Metallurgical and Energy Engineering, Kunming University of Science and Technology, Kunming 650093, China
* Correspondence: zhuxing@kust.edu.cn

Highlights:

What are the main findings?

- A styrene yield of 91.4% was found for 10% k/CeO_2 at 500 °C and CO_2-O_2 mixed atmosphere. The excellent catalytic performance of 10% k/CeO_2 is attributed to the alkali metal oxide modified cerium oxide and carbon dioxide induced oxygen vacancies to promote the dehydrogenation of ethylbenzene.

What is the implication of the main finding?

- The proposed ODH strategy by using oxygen vacancies enriched catalysts offers an important insight into the efficient dehydrogenation of ethylbenzene at mild conditions.

Abstract: Oxidative dehydrogenation (ODH) is an alternative for styrene (ST) production compared to the direct dehydrogenation process. However, ODH with O_2 or CO_2 suffers from either over-oxidation or endothermic property/low ethylbenzene conversion. Herein, we proposed an ODH process with a CO_2-O_2 mixture atmosphere for the efficient conversion of ethylbenzene (EB) into styrene. A thermoneutral ODH is possible by the rationalizing of CO_2/O_2 molar ratios from 0.65 to 0.66 in the temperature range of 300 to 650 °C. K modification is favorable for ethylbenzene dehydrogenation, and 10%K/CeO_2 achieved the highest ethylbenzene dehydrogenation activity due to the enhanced oxygen mobility and CO_2 adsorbability. The catalyst achieved 90.8% ethylbenzene conversion and 97.5% styrene selectivity under optimized conditions of CO_2-$4O_2$ oxidation atmosphere, a temperature of 500 °C, and a space velocity of 5.0 h^{-1}. It exhibited excellent catalytic and structural stability during a 50 h long-term test. CO_2 induces oxygen vacancies in ceria and promotes oxygen exchange between gaseous oxygen and ceria. The ethylbenzene dehydrogenation in CO_2-O_2 follows a Mars-van Krevelen (MvK) reaction mechanism via Ce^{3+}/Ce^{4+} redox pairs. The proposed ODH strategy by using oxygen vacancies enriched catalysts offers an important insight into the efficient dehydrogenation of ethylbenzene at mild conditions.

Keywords: ethylbenzene; oxidative dehydrogenation; ceria; CO_2

check for updates

Citation: Sun, H.; Zhang, J.; Li, K.; Wang, H.; Zhu, X. Efficient Oxidative Dehydrogenation of Ethylbenzene over K/CeO_2 with Exceptional Styrene Yield. *Catalysts* **2023**, *13*, 781. https://doi.org/10.3390/catal13040781

Academic Editor: Carl Redshaw

Received: 28 March 2023
Revised: 12 April 2023
Accepted: 13 April 2023
Published: 21 April 2023

1. Introduction

Styrene was an important organic raw material for the production of plastics and synthetic rubber [1]. By the end of 2021, the global total styrene production capacity was close to 39.8 million tons/year, and that of China was 14.789 million tons/year. China has become the largest styrene production country in the world. At present, the catalytic dehydrogenation process of ethylbenzene accounts for about 90% of the global styrene production. However, it still suffers from challenges including the high feed ratio of steam to ethylbenzene, the limited conversion rate by thermodynamic equilibrium, complicated product separation, etc., which leads to high energy consumption [1]. Therefore, the

development of a new process to improve the production efficiency of styrene and solve the problems existing in the catalytic dehydrogenation process of styrene is urgently required.

In recent years, researchers have focused on the ethylbenzene ODH with O_2 [2–5], N_2O [6–8] and CO_2 [9–19] as oxidants. The advantage of ethylbenzene ODH is that the hydrogen produced in the reaction process can be completely oxidized into water by the oxidant, which avoids the limitation of the equilibrium conversion rate in traditional dehydrogenation and makes full use of the heat generated in hydrogen combustion, thus reducing the process energy consumption [1]. Ethylbenzene ODH with CO_2 as an oxidant could convert CO_2 into CO while dehydrogenating, which could inhibit the deep oxidation of hydrocarbons and provide a new way for the preparation of styrene and the resource utilization of CO_2. At present, the active catalysts for the ODH reaction of CO_2 ethylbenzene were mainly doped/mixed oxides of Fe [20,21], V [22,23], Co [24], Ce [10,16,25,26], Mn [27], and Ti [28]. CO_2 ethylbenzene ODH follows the Mars-van Krevelen redox mechanism [23], but CO_2 activation as a mild oxidant and/or oxygen transfer agent faced obvious challenges in heterogeneous catalysis due to its high kinetic inertia and thermodynamic stability [29,30]. The consumed surface lattice oxygen could not be effectively replenished, which led to the loss of active sites and the deactivation of catalysts [31,32]. Therefore, it was crucial to ensure the reversibility of lattice oxygen on the catalyst surface effectively for the stability of the catalyst [9].

CeO_2 reveals excellent oxygen storage/release ability and high activity in ethylbenzene ODH because of its rapid Ce^{4+}/Ce^{3+} redox cycle [25,26]. It was reported that CeO_2 exhibited significant activity in ethylbenzene ODH with O_2 [33]. However, due to the safety problems and excessive oxidation of O_2, the selectivity of styrene remained low. The ODH reaction of ethylbenzene using CO_2 as an oxidant was effective in improving the yield of styrene and inhibiting the deposition of coke. In a CO_2 atmosphere, the consumed lattice oxygen could not be effectively replenished. Therefore, O_2 was combined with CO_2 to replenish the consumed lattice oxygen of CeO_2, thus promoting the ethylbenzene conversion in the ODH reaction. Currently, the oxidative dehydrogenation of ethylbenzene using CO_2-O_2 remains unknown. Besides, it was also reported that LaSrFe promoted by alkali metal Li/Na/K could significantly improve the product selectivity of ODH by the modification of lattice oxygen [34]. CeO_2 could improve the catalytic activity of the Fe_2O_3-K_2O-based catalyst, accelerating the formation of styrene [35]. Thus, it is expected that the modification of CeO_2 using alkali metals (Li/Na/K) might promote the ethylbenzene conversion in ODH in a mixed atmosphere of CO_2-O_2.

In this paper, composite oxide catalysts Li/CeO_2, Na/CeO_2, and K/CeO_2 synthesized by co-precipitation and over-impregnation methods were investigated in the ethylbenzene ODH process to explore the effect of alkali metals' modification on CeO_2. The candidate selected for the catalyst to explore the effect of the oxidants and the reaction temperature was 10%K/CeO_2. In combination with the surface composition and microstructure of the catalyst, the reaction pathway of ethylbenzene over the 10%K/CeO_2 catalyst was clarified further. The 10%K/CeO_2 catalyst exhibited excellent ODH activity and stability in a CO_2-O_2 mixed atmosphere at 500 °C. The reaction of ethylbenzene with O_2 was the main reaction, and the reaction of ethylbenzene with CO_2 was the auxiliary reaction with the following equations.

$$C_8H_{10} + 0.5\ O_2 = C_8H_8 + H_2O \quad (1)$$

$$C_8H_{10} + CO_2 = C_8H_8 + CO + H_2O \quad (2)$$

The proposed ceria-based catalyst and novel ODH process might offer a new insight into the improvement of ethylbenzene conversion with high styrene selectivity.

2. Results and Discussion

2.1. Theoretical Analysis of Thermoneutral Oxidative Dehydrogenation

Currently, most CO_2/EB in CO_2 ethylbenzene ODH is >10:1 [9,18,22,25,36], and the high CO_2 usage led to the complicated subsequent product separation and low ethylbenzene conversion. It has been reported that O_2 ethylbenzene ODH was an exothermic reaction with high ethylbenzene conversion, but it suffers from over-oxidation and low selectivity [2]. CO_2 ethylbenzene ODH is a heat-absorbing reaction which can avoid deep oxidation and achieve high styrene selectivity, but low ethylbenzene conversion [25]. If the CO_2-O_2 mixed atmosphere is used as the oxidant for EB ODH, it will achieve the goals of reducing the amount of CO_2, simplify the product separation, improve the conversion of ethylbenzene, and reduce the energy consumption of the reaction. If this solution is feasible, it will be of great significance for the study of mixed oxidants for EB-ODH.

The enthalpy changes of the reaction of ethylbenzene with CO_2 or O_2 alone was simulated by integrating the heat absorption and exotherm of the reaction. As shown in Figure 1, the specific heat uptake/exhaustion values of the enthalpy change of the reaction of ethylbenzene with CO_2 or O_2 alone, and the enthalpy change of the reaction of both was within one order of magnitude, and the simulation that resulted provided theoretical data support for the reaction of the CO_2-O_2 mixed atmosphere with ethylbenzene to reach the thermoneutral condition.

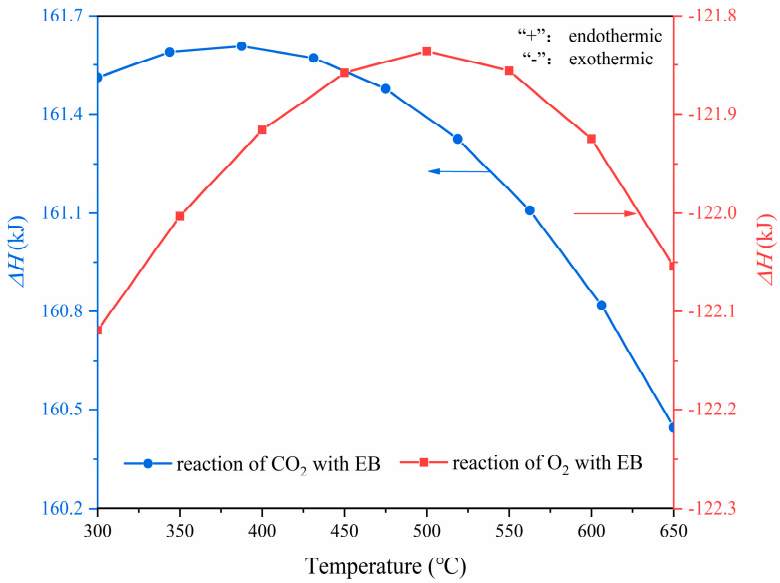

Figure 1. Enthalpy change of the reaction of CO_2 or O_2 with ethylbenzene ODH at different temperature conditions obtained by HSC software simulation.

In order to reduce the energy consumption of CO_2 ethylbenzene ODH, the enthalpy change of the reaction between CO_2/O_2 and ethylbenzene ODH was simulated in HSC by using a fixed molar amount of CO_2. In combination with O_2-ODH and CO_2-ODH, an enthalpy change $\Delta H = 0$ (dynamically 0) will be obtained to achieve an ideal thermoneutral condition. The ratios of each reactant obtained are shown in Table 1. The results showed that it was feasible to achieve the theoretical thermoneutral conditions for the reaction of the CO_2-O_2 mixed atmosphere with ethylbenzene ODH. It shows that O_2-to-CO_2 molar ratios that ranged from 0.65 to 0.66 are able to achieve a thermoneutral condition. The reaction equation under mixed atmosphere at 500 °C is:

$$2.3254\ C_8H_{10}\ (g) + CO_2\ (g) + 0.6627\ O_2\ (g) = 2.3254\ C_8H_8\ (g) + CO\ (g) + 2.3254\ H_2O\ (g) \quad (3)$$

Table 1. Ratio of molar amounts of each reactant required for the enthalpy change ΔH = 0 for the reaction with EB oxidative dehydrogenation under the mixed atmospheric conditions of CO_2 and O_2.

Temperature (°C)	XC_8H_{10} (g) + CO_2 (g) + YO_2 (g) = XC_8H_8 (g) + CO (g) + XH_2O (g)			
	EB (mol)	CO_2 (mol)	O_2 (mol)	Δ*H* (kJ) (Dynamic to 0)
300	2.3226	1	0.6613	0
350	2.3245	1	0.6622	0
400	2.3256	1	0.6628	0
450	2.3259	1	0.6629	0
500	2.3254	1	0.6627	0
550	2.3239	1	0.6619	0
600	2.3214	1	0.6607	0
650	2.3176	1	0.6588	0

2.2. *Synthesis of K/CeO$_2$ Catalyst*

2.2.1. Effect of Alkali Metals Modification on CeO_2

The reaction performance of alkali metal Li/Na/K loaded CeO_2 catalysts were evaluated by EB-TPR experiments. Figure 2a shows the XRD patterns of CeO_2 with different alkali metals loaded (X = Li/Na/K), with the surface loading of CeO_2 by Li/Na/K. There was no obvious shift for the characteristic peaks of CeO_2 (PDF 78-0694), which indicated that the loading of alkali metals did not change the crystalline phase of CeO_2. The peaks corresponding to Li/Na/K oxides were also not observed in the XRD patterns, suggesting that the oxides of alkali metals were evenly distributed on the CeO_2 surface. The intensity of the characteristic peaks for the Li-loaded CeO_2 was larger than that of all other samples, which meant the grain size of CeO_2 became larger after Li was loaded.

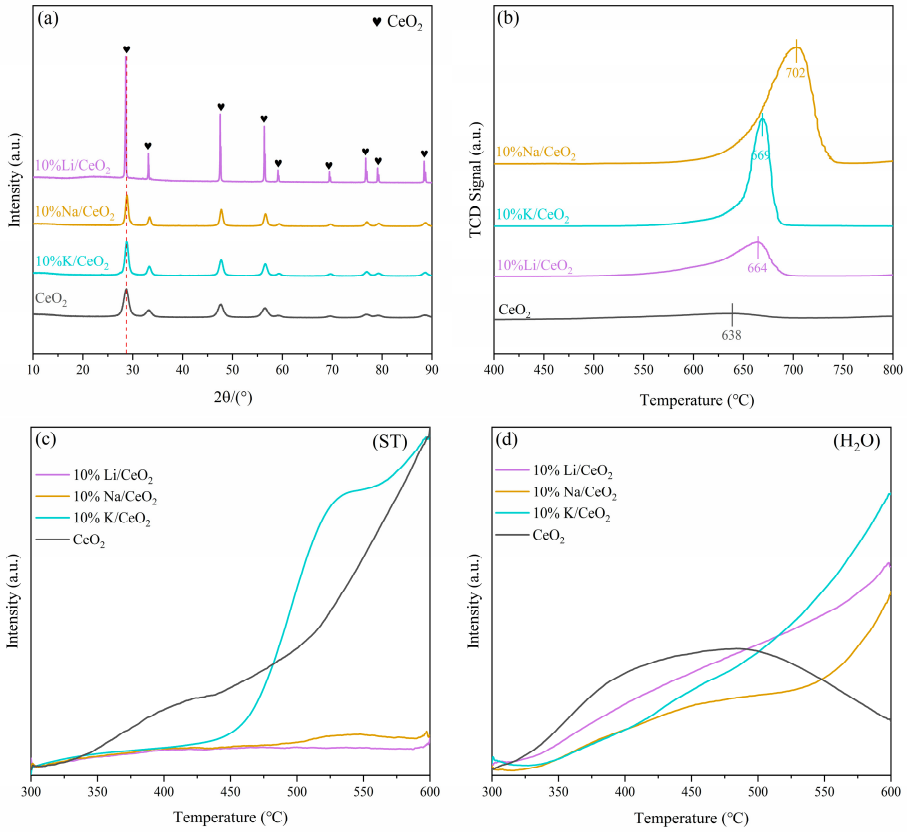

Figure 2. (**a**) XRD, (**b**) H_2-TPR, (**c**) styrene (ST) and (**d**) H_2O mass spectra of EB-TPR (reaction conditions: ramp rate 10 °C/min, T_{EB} = 25 °C, space velocity = 7.5 h^{-1}) for 10%X/CeO_2 (X = Li, Na, K).

The reduction ability of CeO_2 with different alkali metal modifications was tested for H_2-TPR, as shown in Figure 2b. At 638 °C, the reduction peak for CeO_2 was due to the reduction of lattice oxygen [37,38]. The reduction peak area and the intensity of Li/Na/K loaded CeO_2 was much stronger than CeO_2. It illustrated that the amount of reducible oxygen was increased after alkali metal modification, which corresponded to the significant enhancement in the amount of lattice oxygen [13]. This also demonstrated that the loading of alkali metals could greatly enhance the oxygen storage capacity of the catalyst.

Figure 2c showed the styrene generation in EB-TPR (EB-temperature program reduction) experiment at 300–600 °C. As shown in the results, styrene started to be generated at 350 °C on the pure CeO_2, and the generation amount of styrene was increased rapidly after the temperature reached 500 °C. For 10%K/CeO_2, it started to generate styrene from 400 °C. Styrene's generation performance increased sharply after the temperature reached 450 °C, while the styrene generation rate slowed down after 550 °C. In contrast, there was almost no styrene generation on the Li/Na modified CeO_2. This showed that the oxygen storage capacity was not a decisive factor to enhance the catalytic activity. Figure 2d shows that 10%K/CeO_2 exhibited a strong rising trend of the H_2O mass spectrum after 450 °C. Combined with the rising trend of the CO_2 mass spectrum (Figure S1), this suggests that the lattice oxygen release rate of 10%K/CeO_2 was accelerated by the increase in reaction temperature, which led to the partial oxidation. Therefore, it was necessary to select a suitable reaction temperature to reduce the excessive oxidation of EB on the catalyst. These results reveal that the doping of the alkali metal Li/Na/K to the CeO_2 surface could greatly improve its oxygen storage capacity.

From Figure 3a, the amount of styrene generation was gradually increased at 500 °C with the reaction proceeds. Figure 3b shows the product distribution of the oxidative dehydrogenation of ethylbenzene. The generation amounts of by-products on 10%Li/CeO_2 were the highest, with only 54.5% styrene selectivity and 17.3% ethylbenzene conversion. The styrene selectivity of 10%Na/CeO_2 could reach 86.9%, while ethylbenzene conversion was only 29.0%. The best catalytic performance was from 10%K/CeO_2 with 92.4% styrene selectivity and 71.9% ethylbenzene conversion. The catalytic performance of ethylbenzene oxidative dehydrogenation was related to the type of alkali metal. CeO_2, with the doping of Li and Na, suffered from a serious decrease in catalytic performance and an increase in excessive oxidation. Therefore, alkali metal K was chosen for the surface modification of CeO_2 to further improve the catalytic performance.

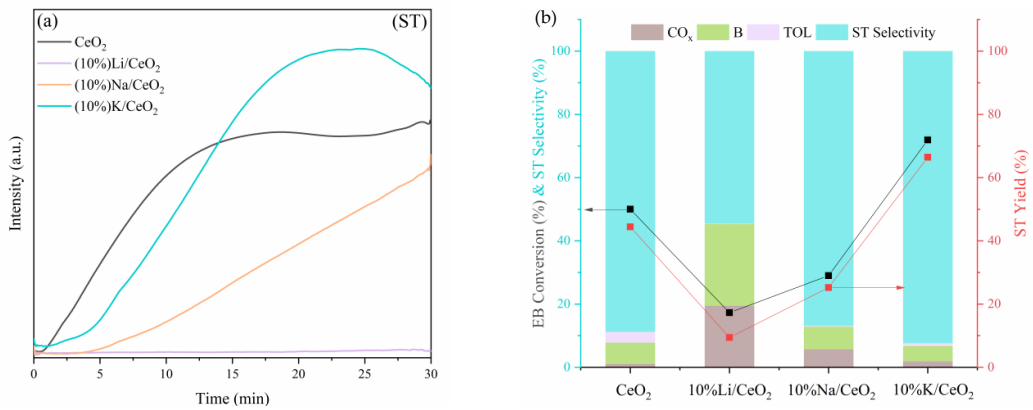

Figure 3. Catalytic performance of alkali metal Li/Na/K modified CeO_2. (**a**) styrene (ST) mass spectra of 10%X/CeO_2; (**b**) product distribution of 10%X/CeO_2 at 500 °C (X = Li, Na, K). Experimental conditions: temperature rise rate 10 °C/min, T_{EB} = 25 °C, flow rate 25 mL/min, atmosphere Ar, catalyst dosage 500 mg, space velocity = 7.5 h^{-1}.

2.2.2. Effect of K Loading Amounts on CeO_2

Figure 4a indicates the XRD pattern of the K/CeO_2 catalyst with different loading K content. As Figure 4a shows, the catalysts of CeO_2 and n%K/CeO_2 (n = 5, 10, 15, 20) appeared at the CeO_2 characteristic diffraction peaks (PDF 78-0694), which indicates that

all of the catalysts are mainly of CeO_2 phase with a fluorite structure. The diffraction peak of the phase associated with potassium was not detected either because potassium is uniformly distributed on the surface of CeO_2, or the loading did not reach the detection limit of XRD.

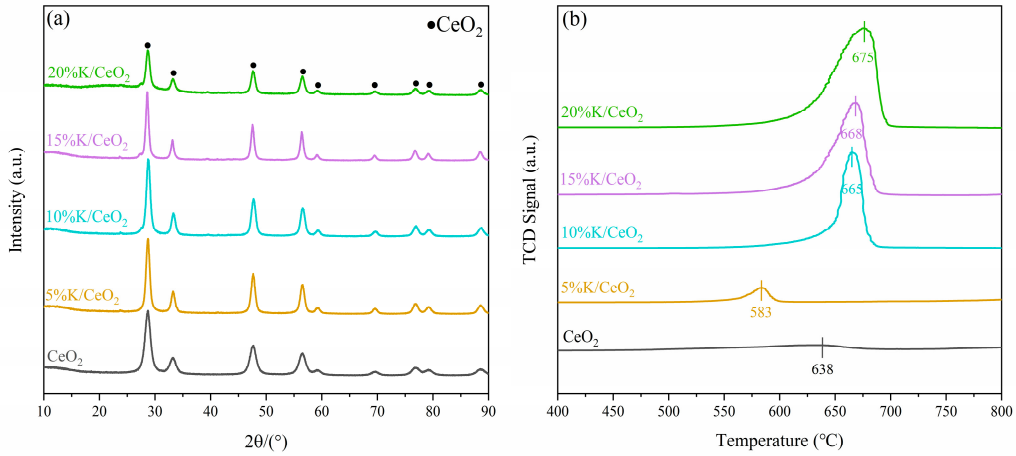

Figure 4. Characterization of n%K/CeO_2. (**a**) XRD; (**b**) H_2-TPR (n = 0, 5, 10, 15, 20).

The H_2 temperature programmed reduction (H_2-TPR) test was performed to detect the reducibility of the CeO_2 and n%K/CeO_2. The H_2-TPR curves are shown in Figure 4b. The curve of CeO_2 was one reduction peak at 638 °C, which was ascribed to the reduction of the CeO_2 surface lattice oxygen [13,37,38]. When a small amount of K was loaded (5%K/CeO_2), the reduction peak at 638 °C shifted to a lower temperature (583 °C), and the intensity of the peak increased slightly. Compared to the pure CeO_2, the reduction temperature of the surface lattice oxygen rose by about 30 °C for the 10%K/CeO_2 catalyst, but the peak intensity was significantly increased. The results suggest that the K modification of CeO_2 promoted the release of the CeO_2 surface lattice oxygen and the following hydrogen consumption. The temperature of the reduction peak at 638 °C increases continuously with the K loading. However, the amount of hydrogen consumption did not obviously add as well as temperature did. The explanation may be that the overloading of potassium led to the enhanced interaction between K_2O and CeO_2, which inhibited the release of the surface lattice oxygen. The H_2-TPR results show that the catalytic performance of K/CeO_2 in the oxidative dehydrogenation of ethylbenzene can be promoted only when the appropriate amount of K was loaded.

The basicity of the catalyst surface plays a key role in the activation of ethylbenzene C-H with CO_2 during ethylbenzene ODH. The CO_2 temperature programmed desorption (CO_2-TPD) was conducted to test the surface basicity of the n%K/CeO_2 catalysts, as shown in Figure 5. For the pure CeO_2, the CO_2 desorption peak appeared at temperatures between 70–200 °C, which was assigned to the weak base site. After loading the alkaline metal potassium, the CO_2 desorption peak was detected between temperatures of 600–700 °C. As expected, the K loading increased the alkaline sites on the K/CeO_2 catalyst surface [39]. The 10%K/CeO_2 has the strongest desorption peak, which indicates that the 10%K/CeO_2 catalyst reveals the strong adsorption and desorption capacity of CO_2, which might be the beneficial ethylbenzene conversion.

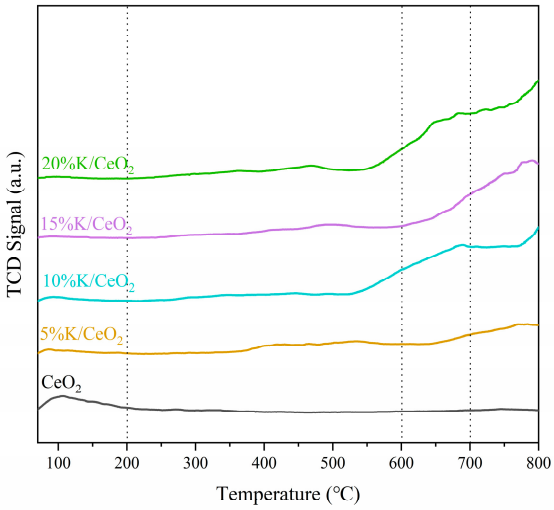

Figure 5. CO_2-TPD with different ratios of K surface modified CeO_2.

TEM was used to observe the effect of K loading on the morphology of CeO_2. As shown in Figure 6a–c, both K modified and unmodified CeO_2 reveal an irregular polygonal structure, which was consistent with the XRD test results. Lattice fringes with d values of 0.19 nm and 0.27 nm were observed on the 10%K/CeO_2 and 20%K/CeO_2 catalysts, corresponding to the (311) and (200) crystal planes of K_2O, respectively. This indicated that K was uniformly distributed on the surface of CeO_2 in the form of K_2O, while the heavy load of K made the interaction between K_2O and CeO_2 too strong, which was not conducive to the release of surface lattice oxygen. This further conformed the detection results of H_2-TPR. Therefore, an appropriate load of K might be conducive to the ethylbenzene ODH.

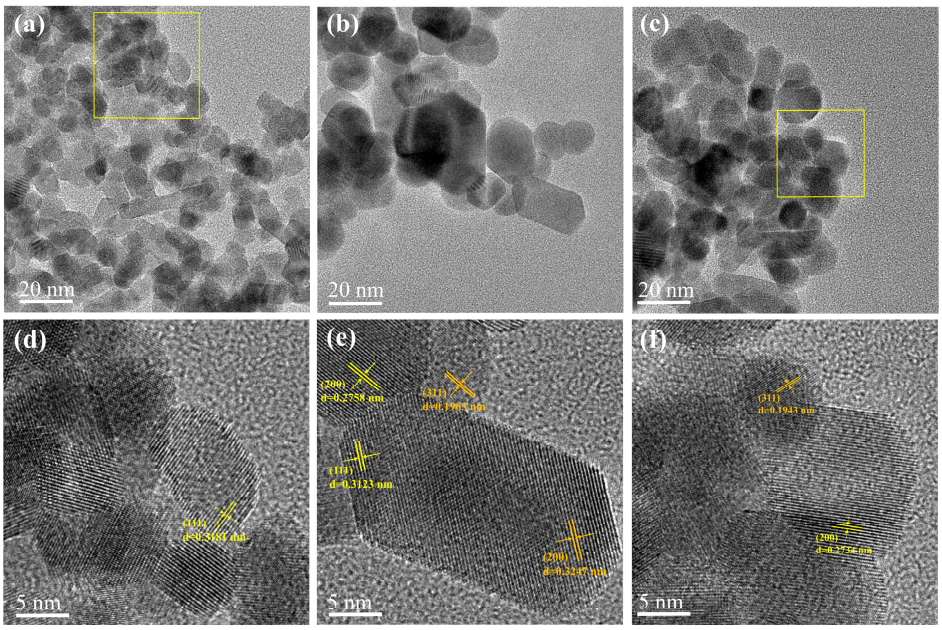

Figure 6. HRTEM of fresh samples (**a**,**d**) for CeO_2; (**b**,**e**) for 10%K/CeO_2; (**c**,**f**) for 20%K/CeO_2.

In order to study the effect of K loading on the reactivity of K/CeO_2 catalysts, the ethylbenzene dehydrogenation tests were conducted at 500 °C. Figure 7a shows the mass spectrum trends of styrene production over the K/CeO_2 catalyst with different K loading amounts. The production rate of styrene at 10%K/CeO_2 was significantly higher than that of other catalysts after 5 min of reaction, and reached a peak at about 25 min. As seen in the product distribution diagram of each catalyst in Figure 7b, 10%K/CeO_2 shows the

highest dehydrogenation activity among all samples, achieving a high styrene yield of 71.9%. Combined with the above characterization, it might be speculated that surface K_2O is conductive to ethylbenzene activation and enhanced dehydrogenation activity. In the industrial ethylbenzene dehydrogenation process, surface K species in the commercial K-Fe-O catalysts have been found to promote the formation of $KFeO_2$ in the active phase from iron oxide, while K^+ ions promoted the polarization of Fe-O bonds and enhanced the alkalinity of the active center [40], after which they enhanced the selectivity of styrene.

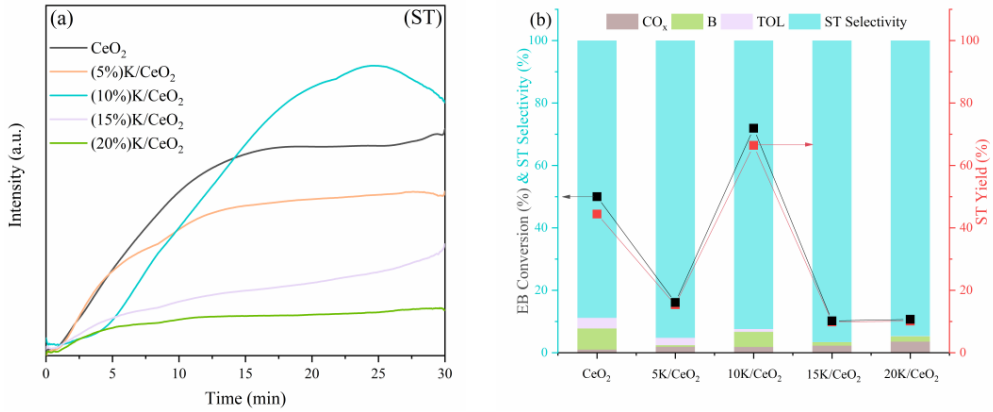

Figure 7. EB catalytic performance of CeO_2 doped with different ratios of alkali metal K. (**a**) styrene (ST) mass spectra of n%K/CeO_2 at 500 °C; (**b**) product distribution of n%K/CeO_2 at 500 °C (n = 0, 5, 10, 15, 20). Experimental conditions: temperature rise rate 10 °C/min, T_{EB} = 25 °C, flow rate 25 mL/min, atmosphere Ar, catalyst dosage 500 mg, space velocity = 7.5 h^{-1}.

2.3. Ethylbenzene ODH Performance

2.3.1. Optimization of Reaction Conditions in ODH

The effect of oxidants on the ODH performance over 10%K/CeO_2 was investigated, as shown in Figure 8. In the CO_2 atmosphere (orange icon), the high ethylbenzene conversion at 80% and styrene selectivity (>95%) were obtained at CO_2 excess coefficients of $3CO_2$ and $4CO_2$. In the O_2 (red icon) atmosphere, high reactivity was obtained at O_2 excess coefficients of $4O_2$. However, the styrene selectivity remained relatively low compared with the CO_2 atmosphere. This is because that, as a strong oxidant, higher oxygen partial pressure is conducive to ethylbenzene conversion, but it will also lead to excessive oxidation and reduce styrene selectivity [41,42]. According to Hongbo et al. the lattice oxygen released within the catalyst controls the reaction process, the C_3H_8 conversion decreases with decreasing oxygen concentration, and the selectivity of C_3H_6 increases due to decreasing peroxidation [43]. In Figure 8, CO_2-$4O_2$, $3CO_2$-$4O_2$ and $4CO_2$-$4O_2$ all have stable and efficient ethylbenzene conversion due to the high oxygen partial pressure provided by $4O_2$. Conversely, as a soft oxidant, CO_2 will inhibit excessive oxidation and thus improve styrene selectivity, but with relatively low ethylbenzene conversion.

Considering the advantages of O_2 and CO_2 oxidants in ODH, the dehydrogenation performance of the CO_2-O_2 mixture (Blue icon) was studied as oxidants in ODH over the 10%K/CeO_2 catalyst. Among them, CO_2-$4O_2$ shows the highest dehydrogenation activity with 90.8% ethylbenzene conversion and 97.5% styrene selectivity due to the synergistic effect of CO_2 and O_2. On the one hand, CO_2 dilutes the O_2 concentration, thus suppressing the excessive oxidation and improving styrene selectivity. On the other hand, O_2 in CO_2 enhances ethylbenzene conversion in the CO_2 atmosphere.

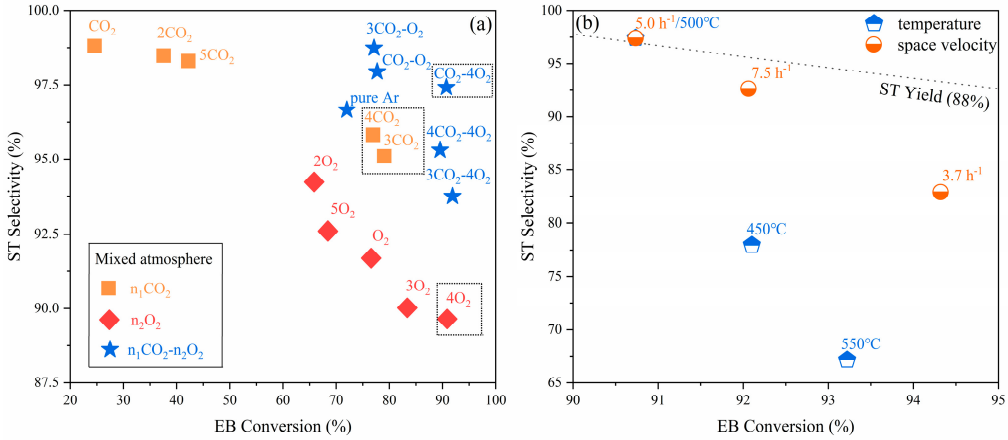

Figure 8. EB-ODH performance (**a**) in various atmospheres, with the following experimental conditions: reaction temperature 500 °C, T_{EB} = 25 °C, reaction time 5 h, flow rate 25 mL/min, atmosphere CO_2/Ar, O_2/Ar, CO_2-O_2/Ar, catalyst dosage 1000 mg, space velocity = 5.0 h^{-1}; (**b**) under different temperature and space velocities, different temperature experimental conditions: T_{EB} = 25 °C, reaction time 5 h, flow rate 25 mL/min, atmosphere 1CO_2-4O_2, catalyst dosage 1000 mg, space velocity = 5.0 h^{-1}; space velocities experimental conditions: reaction temperature 500°C, T_{EB} = 25 °C, reaction time 5 h, flow rate 25 mL/min, atmosphere 1CO_2-4O_2. The CO_2 excess coefficients (n) represent the multiplication of the increase in the molar amount of CO_2 compared to the thermoneutral conditions in Table 1. The O_2 excess coefficients (n) and the excess coefficients (n) for a mixed CO_2-O_2 atmosphere are defined similarly to the CO_2 excess coefficients.

Combined with the mass spectrum curves of CO, H_2O and O_2 (Figure S2), EB-ODH with O_2 (Equation (1)) in a CO_2-4O_2 atmosphere is the main reaction which dominates ethylbenzene dehydrogenation to generate styrene, while EB-ODH with CO_2 (Equation (2)) in a CO_2-4O_2 atmosphere is the secondary reaction which reduces the concentration of O_2 and suppresses excessive oxidation. Figure 8b compares the EB-ODH performance of 10%K/CeO_2 under the CO_2-4O_2 atmosphere at different temperatures and space velocities. It is obvious that 10%K/CeO_2 shows the highest dehydrogenation activity in the CO_2-4O_2 atmosphere, following with 90.8% ethylbenzene conversion and 97.5% styrene selectivity under 500 °C and 5.0 h^{-1} space velocities.

2.3.2. Reaction Stability

The long-term stability of the 10%K/CeO_2 catalyst was tested under the optimal experimental conditions of CO_2-4O_2, a reaction temperature of 500 °C, and a space velocity of 5.0 h^{-1} for 50 h, as shown in Figure 9. The average ethylbenzene conversion and styrene selectivity remain at approximately 96.1% and 94.2%, respectively. In a 50 h long-term stability test, the styrene yield reaches as high as 91.4%. The 10%K/CeO_2 catalyst exhibited excellent activity and stability in the 50 h long-term test, which was clearly superior to the ODH performance reported in the available literature [10,12,15,25,26,44]. Furthermore, a slight decrease in the conversion of ethylbenzene of about 2% was observed after the reaction reached 43 h.

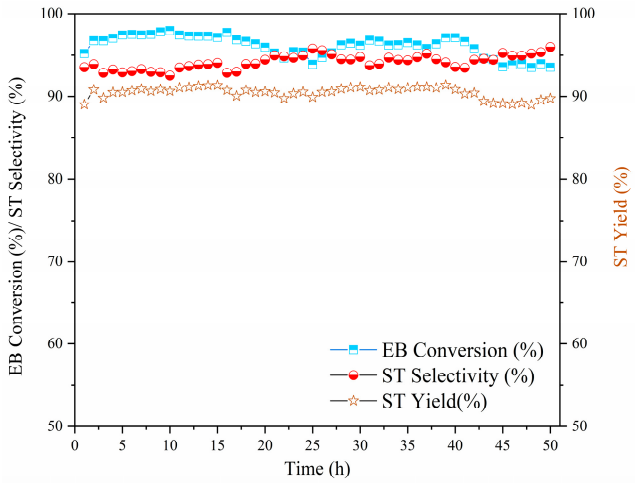

Figure 9. Stability test of 10%K/CeO_2. Reaction conditions: 500 °C, flow rate 25 mL/min, mixed atmosphere CO_2-$4O_2$, space velocity 5.0 h^{-1}.

The XRD and H_2-TPR were conducted to investigate the evolution of the structure and reducibility of the catalyst before and after the 50 h stability test. Figure 10a shows the XRD plots of the samples before and after the 50 h stability test for 10%K/CeO_2. In Figure 10a, the characteristic peaks of CeO_2 (PDF 78-0694) were observed for both the fresh and spent catalyst. The intensity of the main diffraction peaks of the spent catalyst were increased after the stability test, suggesting the crystallization of ceria. Furthermore, a weak diffraction peak at 2θ = 31.8° corresponding to K_2CO_3 was observed for the spent catalyst. The formation of carbonate on the surface of ceria might lead to a slight decrease of ethylbenzene conversion in a long-term stability test. Figure 10 shows that one weak reduction peak was observed at 563 °C for the spent catalyst, corresponding to the reduction of Ce^{4+} on the surface. Compared to fresh catalyst, the reduction peak was obviously decreased and shifted to higher temperature due to the decreased reducibility. This will be ascribed to the formation of carbonate on the surface of ceria, which hindered oxygen mobility and donation ability.

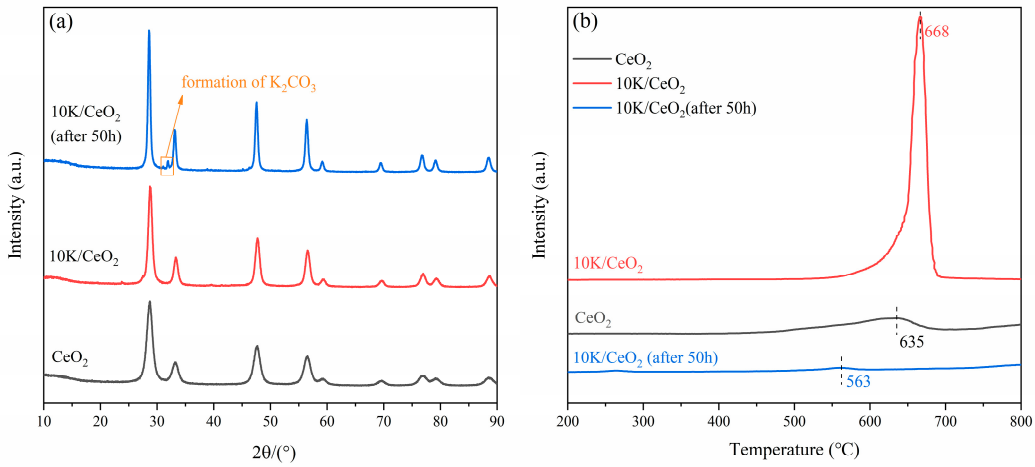

Figure 10. Sample characterization before and after stability testing of 10%K/CeO_2. (**a**) XRD and (**b**) H_2-TPR.

Figure 11 shows the TEM and EDS images of the spent catalyst after the 50 h stability test. As shown in Figure 11a, both the fresh and spent catalyst are composed of hexagonal crystals with a size of approximately 40 nm. CeO_2 mainly exposes the (111) crystalline surface and K_2O mainly exposes the (200) crystalline surface. After the long-term stability test, the boundary of ceria grain was corroded and the grain grew bigger compared to

fresh ones due to the slight sintering of material in ODH (Figure S3). The EDS mapping suggests that all elements (Ce, O and K) are well dispersed and no obvious agglomeration was observed. The Ce distribution is well-matched with the morphology of ceria grain in the catalyst, while K tends to disperse in a large region. This reveals that K_2O or K_2CO_3 are dispersed on the surface of ceria grain. Those results confirmed the high structural stability during the ODH process.

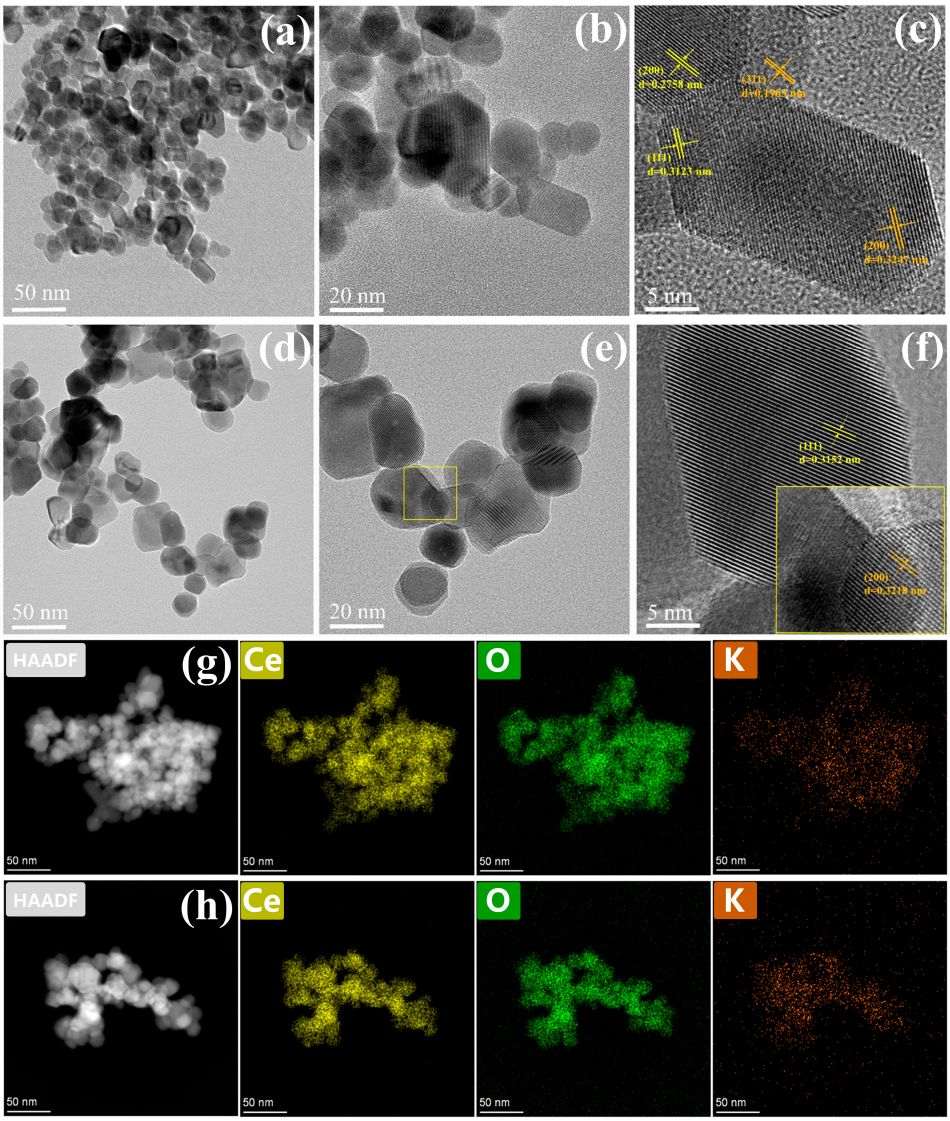

Figure 11. HRTEM and EDS of 10%K/CeO_2 before and after a 50 h stability test. (**a**–**c**) HRTEM of fresh 10%K/CeO_2; (**d**–**f**) HRTEM of 10%K/CeO_2 after a 50 h stability test; (**g**) EDS of fresh 10%K/CeO_2; (**h**) EDS of 10% EDS of K/CeO_2.

2.4. Surface Reaction Mechanism

The surface reaction of ethylbenzene over the 10%K/CeO_2 catalyst was explored by a temperature programmed surface reaction equipped with a Fourier transform infrared spectrometer. In Figure 12a, several band features of ethylbenzene were observed after the adsorption of ethylbenzene/Ar flow at 100 °C. The bands at 3040 and 3020 cm^{-1} correspond to the C-H extension in the aromatic ring. The bands at 2980 and 2940 cm^{-1} correspond to methyl and methylene in ethyl. The band at 1600 cm^{-1} was ascribed to the skeletal C-C stretching pattern of the aromatic ring. All of those bands suggest that ethylbenzene was absorbed on the surface of the catalyst. In Figure 12b, the very weak band corresponding to the vinyl overtone was observed at 1760 cm^{-1}, which reveals that

ethylbenzene was dehydrogenated into styrene [25] at temperatures as low as 200 °C. The bands of surface CO_2 and carbonate were observed, which might be ascribed to the full oxidation of hydrocarbons or adsorption from ambient CO_2. According to the band feature at 200 °C, ethylbenzene was absorbed on the surface the catalyst, and then reacted with surface absorbed gaseous oxygen to produce styrene and/or complete oxidation products (H_2O and CO_2). The reaction behaviors of ethylbenzene on the surface of the catalysts are similar under different oxidation atmospheres.

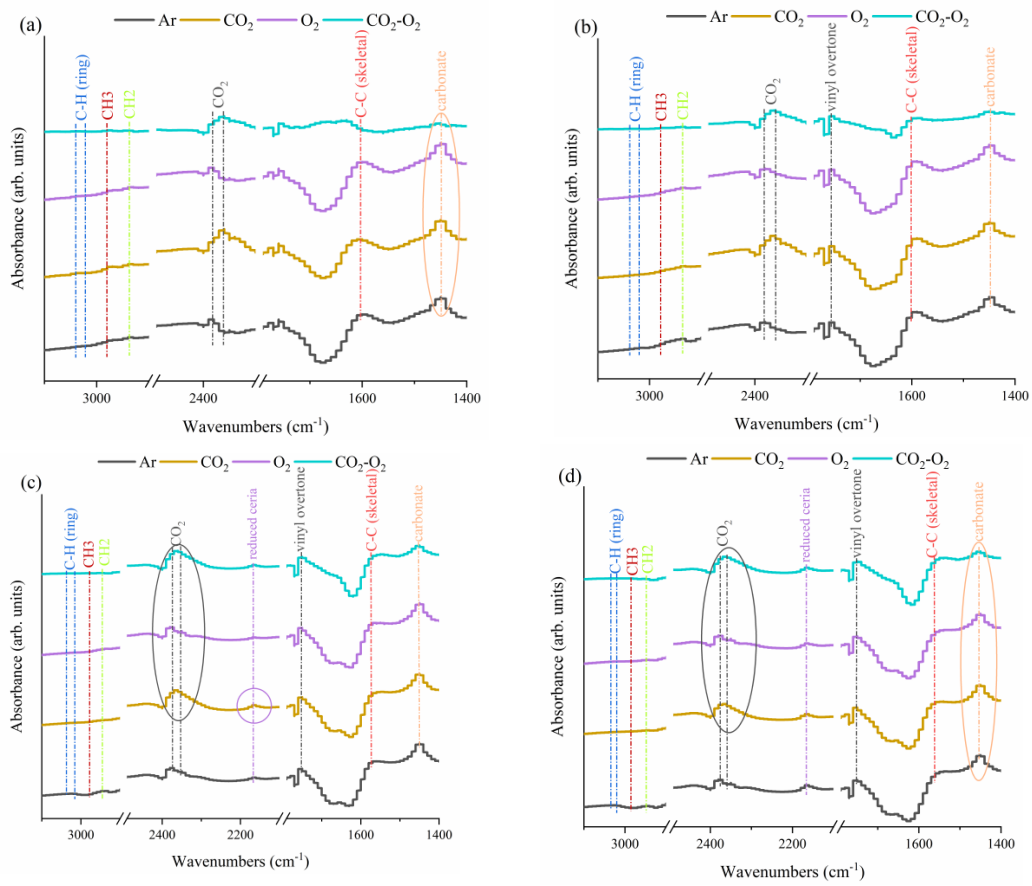

Figure 12. In situ IR spectra of the programmed warming of ethylbenzene over the 10%K/CeO_2 catalyst under different atmospheres. (**a**) 100 °C; (**b**) 200 °C; (**c**) 400 °C; (**d**) 500 °C. Experimental conditions: a warming rate 10 °C/min, an adsorption temperature of 100 °C, an adsorption time of 30 min, purge gas Ar, purge flow rate 25 mL/min, four atmospheres: pure Ar, CO_2, $4O_2$, CO_2-$4O_2$, and the 10%K/CeO_2 catalyst, respectively.

The appearance of reduced cerium bands (corresponding to Ce^{3+} and oxygen vacancies) was observed at different oxidizing atmospheres starting from 400°C. In addition, the peak of the reduced cerium is stronger than the others (O_2 and Ar) in both the CO_2 and CO_2-O_2 atmospheres, indicating that more oxygen vacancies were generated in these two atmospheres. CeO_2 with higher oxygen kinetics promotes the oxidation of carbonate, and there is an inhibitory effect on the formation of carbonate which promotes the reaction; the dehydrogenation of alkanes occurs on the CeO_2 surface and subsequently generates oxygen vacancies on the CeO_2 surface. The role of CeO_2 lattice oxygen in the partial oxidation of the reaction is crucial for oxidative dehydrogenation [45]. O_2, the main force of CeO_2 lattice oxygen supplementation, formed less oxygen vacancies on the CeO_2 surface than CO_2 and the mixed CO_2-O_2 atmosphere, indicating that CO_2 has an induced effect on the formation of oxygen vacancies on the CeO_2 surface. With the increasing reaction temperature, the band of reduced ceria at 500 °C became stronger with a similar intensity of the catalysts under four atmospheres due to the enhanced oxygen mobility at elevated temperatures.

The induced oxygen vacancies in the catalyst will accelerate the consumption of lattice oxygen and the replenishment of oxygen vacancies using O_2 or CO_2, thus improving the dehydrogenation activity, even though CO_2 will combine with K_2O to produce some carbonates on the surface of ceria. The catalyst retained its high activity in the CO_2-O_2 atmosphere. In this CO_2-O_2 mixture, it can be predicted that oxygen vacancies are the driving force of oxygen exchange during ODH, while O_2 is the main oxygen source for lattice oxygen replenishing. CO_2 plays a very important role in inducing oxygen vacancies and enhancing oxygen exchange during ethylbenzene ODH. It can also be speculated that the ethylbenzene ODH with CO_2-O_2 follows a Mars-van Krevelen reaction mechanism by using Ce^{3+}/Ce^{4+} redox pairs.

3. Materials and Methods

3.1. Materials

Cerium nitrate hexahydrate ($Ce(NO_3)_3{\cdot}6H_2O$, AR), Sodium hydroxide (NaOH, AR), Lithium nitrate ($LiNO_3$, AR), Sodium nitrate ($NaNO_3$, AR), Potassium nitrate (KNO_3, AR), Cetyl trimethyl ammonium bromide (CTAB, AR), Ethylbenzene ($C_6H_5CH_2CH_3$, AR), styrene ($C_6H_5CH_2$, AR), Benzene (C_6H_6, AR), and Toluene ($C_6H_5CH_3$, AR) were purchased from Aladdin Industrial Inc. O_2/Ar (9.99 vol% O_2), CO_2/Ar (5.02 vol% CO_2), high purity Ar (≥99.99 vol% Ar), high purity He (≥99.99 vol% He), and liquid nitrogen were purchased from the Kunming Mercer Gas Co., Ltd. (Kunming, China)

3.2. Catalyst Synthesis

About 4.34 g $Ce(NO_3)_3{\cdot}6H_2O$ and 2.18 g CTAB were dissolved in 200 mL water, and then 300 mL, 0.16 mol·L^{-1} NaOH solution (1.92 g) was added to the above mixture and stirred at 70 °C for 24 h. After stirring, the water bath was aged at 90 °C for 3 h, and then the CTAB was removed by hot filtration to obtain a light yellow solid. The solid was dried at 100 °C for 6 h and then calcined at 600 °C for 4 h in a muffle furnace to obtain CeO_2 samples.

The prepared CeO_2, the different mass percentage nitrate, and 15 mL of deionized water were placed in a 50 mL beaker, placed on a magnetic stirrer at room temperature until the water was completely evaporated, and dried in a 100 °C oven for 6 h. The dried samples were calcined in a muffle furnace at 600 °C for 4 h, ground, pressed, granulated (60–80 mesh) and named n%X/CeO_2 (X means nitrate, X = Li, Na, K; n% means different mass percentages = 5, 10, 15, 20).

3.3. Catalyst Characterization

The phase structure and lattice size of the catalyst were characterized by X-ray diffraction (XRD; D8 Advance, Bruker, Karlsruhe, Germany), where λ was 0.15406 nm, and the tube current and voltage were 40 kV and 30 mA, respectively. The samples were scanned at a scanning rate of 5°/min, and the scanning area was selected from between 10° to 90°.

The Chembet Pulsar automated chemisorption instrument (Pulsar, Quantachrom Instruments, Boynton Beach, FL, USA) was used to study the reducibility of the catalyst by temperature programmed reduction (H_2-TPR). The 50 mg sample was loaded into a quartz reactor, pretreated at 300 °C for 30 min, and then cooled to 50 °C under a continuous flow of Ar (50 mL·min^{-1}). After pretreatment, the temperature was changed from 50 °C to 850 °C at a rate of 10 °C/min in a mixed flow of 10 vol% hydrogen (50 mL·min^{-1}) in argon. The H_2 consumption was recorded by an online thermal conductivity detector (TCD, Quantachrom Instruments, Boynton Beach, FL, USA).

The basicity of the catalyst was studied by CO_2-temperature programmed desorption (CO_2-TPD). The 30 mg sample was placed in a quartz reactor and pretreated at 300 °C for 30 min. The catalyst was then cooled to 100 °C under a continuous flow of Ar (50 mL·min^{-1}). After pretreatment, 10 vol% CO_2 was kept in the mixed flow of Ar (50 mL·min^{-1}) for 30 min. Subsequently, the excess gas was purged with Ar, and the temperature increased from

100 °C to 900 °C at a rate of 10 °C/min. The desorption amount of CO_2 was recorded by TCD.

The morphology and crystallinity of fresh and recycled catalysts were detected by transmission electron microscopy (JEM 2100F, JEOL (Beijing), Beijing, China), and the lattice spacing was detected by high-resolution transmission electron microscopy (JEM 2100F). The element content on the surface of the used catalyst was detected by an energy dispersive spectrometer (EDS, XFlash 5030T, JEOL (Beijing), Beijing, China).

In situ diffuse reflectance infrared Fourier transform spectroscopy (Nicolet iS50 FTIR, Termo Scientific, Waltham, MA, USA) was used to test the changes of functional groups during the reaction. The samples were first loaded into an in situ cell, and the background was collected in an Ar atmosphere at 25 °C. During the temperature-programmed in situ infrared test, the sample was raised to 100 °C in an Ar flow, and ethylbenzene was adsorbed on the sample surface by EB/Ar, EB/(CO_2 + Ar), EB/(O_2 + Ar), and EB/(CO_2 + O_2 + Ar) flow through a room temperature ethylbenzene foaming device for 30 min. The flow of ethylbenzene vapor was then stopped, the gas flow was switched to Ar, and the in situ pool was heated from 100 °C to 500 °C at a rate of 10 °C/min, and the data was recorded every minute. When the isothermal in situ infrared test was carried out at 500 °C, the in situ cell was kept at 500 °C under Ar. Next, the ethylbenzene vapor stream flowed into the in situ cell through the ethylbenzene bubbler at room temperature under Ar, CO_2 + Ar, O_2 + Ar, and CO_2 + O_2 + Ar atmospheres, and the data was recorded every minute.

3.4. Catalytic Performance Testing under Oxygen-Free Conditions

This part of the experiment tested the performance of the catalyst under oxygen-free conditions. The purpose was to test the effect of lattice oxygen on the properties of alkali metal loaded cerium oxide samples. The n%X/CeO_2 was used as the catalyst to carry out the catalytic activity experiment. The experimental device mainly consists of an electric furnace, a multi-directional gas mass flowmeter, an ethylbenzene steam generator, a fixed bed reactor with a temperature controller, a waste gas processor, and an online gas analysis mass spectrometer for gas product analysis. A gas chromatography-mass spectrometry coupler is used to quantitatively study the gas composition of waste gas.

In the isothermal redox test, 500 mg of sample and 100 mg of quartz sand (60–80 mesh) were placed in the reactor and purged with Ar (≥99.99 vol%, 50 mL·min^{-1}) at 200 °C to remove all possible adsorbed impurities. At the beginning of the measurement, the temperature increased from 200 °C to 500 °C at a rate of 10 °C/min. When the temperature reached 500 °C, the gas was switched from Ar to EB/Ar (25 mL·min^{-1}), and the unconsumed EB, styrene (ST), toluene (TOL), benzene (B) and carbon oxide (COX) were recorded and analyzed in real time by MS, and quantified by GC-MS. At the end of the reaction, the reactor was cooled in the Ar environment. EB conversion and styrene selectivity were calculated by the following formula:

$$\text{EB Conversion } (\%) = \frac{N_{EB,in} - N_{EB,out}}{N_{EB,in}} \times 100\% \tag{4}$$

$$\text{ST Selectivity } (\%) = \frac{N_{ST,out}}{N_{B,out} + N_{TOL,out} + N_{COX,out} + N_{ST,out}} \times 100\% \tag{5}$$

where:

$N_{EB,in}$: The amount of EB introduced, mol;
$N_{EB,out}$: The amount of EB emitted, mol;
$N_{ST,out}$: The amount of ST emitted, mol;
$N_{B,out}$: The amount of byproduct B produced by the reaction, mol;
$N_{TOL,out}$: The amount of byproduct TOL produced by the reaction, mol;
$N_{COX,out}$: The amount of byproduct COX produced by the reaction, mol.

3.5. Performance Testing of Oxidative Dehydrogenation of Ethylbenzene

A total of 1000 mg of the sample was placed in the reactor and purged with Ar (gas flow rate 50 mL/min) at 200 °C for 30 min to remove all possible adsorbed impurities. At the beginning of the measurement, the temperature was increased from 200 °C to 500 °C at a heating rate of 10 °C/min. When the temperature reached 500 °C, the gas was switched from Ar to EB/(Ar-CO_2-O_2) (gas flow rate 25 mL/min) for a reaction time of 3 h/5 h/50 h. The unconsumed EB and the ST, TOL, B and COX products were recorded and analyzed by MS every half hour and quantified by GC-MS. At the end of the reaction, the reactor was cooled in Ar. The EB conversion was calculated by Equation (1), and ST selectivity was calculated by the following equation.

$$\text{ST Selectivity } (\%) = \frac{N_{ST,out}}{N_{B,out} + N_{TOL,out} + N_{COX} + N_{ST,out}} \times 100\% \quad (6)$$

N_{COX} is the instantaneous molar amount of carbon oxide. Since the CO_2-O_2 mixed atmosphere was passed into the reactor and the flow rate of CO_2 and O_2 was fixed, there was a base molar amount of CO_2, and when CO_2 was consumed below the base molar amount as the reaction proceeded, the conversion rate of CO_2 was calculated using the following equation.

$$CO_2 \text{ Conversion } (\%) = \frac{N_{CO2,in} - N_{CO2,out}}{N_{CO2,in}} \times 100\% \quad (7)$$

When $N_{CO2,in} > N_{CO2,out}$, $N_{COX} = 0$ (CO_2 was consumed and CO was the reaction product), the CO_2 conversion rate was calculated by Equation (4); When $N_{CO2,in} < N_{CO2,out}$, the reaction process produces CO_2, which was considered to be the by-product CO_X, $N_{COX} = N_{CO2,in} - N_{CO2,out}$ (CO was the reaction product).

4. Conclusions

We proposed an efficient ODH of ethylbenzene into styrene using a K/CeO_2 catalyst under a CO_2-O_2 mixture atmosphere at 500 °C. The thermodynamic analysis illustrates that a thermoneutral ODH is possible by the rationalizing of CO_2/O_2 molar ratios from 0.65 to 0.66 in the temperature range of 300 to 650 °C. The modification of alkali metals (Li, Na and K) oxides could greatly enhance the oxygen storage capacity ceria, and the K modification is favorable for ethylbenzene dehydrogenation. 10%K/CeO_2 reveals the highest oxygen mobility and strong CO_2 adsorbability, achieving the highest ethylbenzene dehydrogenation activity. The catalyst achieved 90.8% ethylbenzene conversion and 97.5% styrene selectivity under the optimized conditions of the CO_2-4O_2 oxidation atmosphere, a temperature of 500 °C, and a space velocity of 5.0 h^{-1}. It maintained high catalytic and structural stability during the 50 h long-term test. The slight crystallization of ceria and some surface carbonates were observed for the spent catalyst. In situ DRIFTS experiments suggested that CO_2 induces oxygen vacancies in ceria and promotes oxygen exchange between gaseous oxygen and ceria. The ethylbenzene ODH with CO_2-O_2 follows a Mars-van Krevelen reaction mechanism by using Ce^{3+}/Ce^{4+} redox pairs. The proposed ODH strategy of using oxygen vacancies enriched catalysts offers an important pathway for the efficient dehydrogenation of ethylbenzene.

Supplementary Materials: The following supporting information can be downloaded at: https://www.mdpi.com/article/10.3390/catal13040781/s1, Figure S1: EB-temperature program reduction; Figure S2: Mass spectra of reactants and products of EB-ODH under mixed atmosphere of CO_2-4O_2; Figure S3: Raman of samples before and after stability testing of 10%K/CeO_2; Table S1: Enthalpy change of reaction at different temperatures; Table S2: Thermoneutral reaction equation.

Author Contributions: Conceptualization, J.Z. and X.Z.; methodology, H.S. and J.Z.; software, H.S.; validation, H.S.; investigation, H.S.; resources, H.W. and K.L.; data curation, H.S.; writing—original draft preparation, H.S.; writing—review and editing, J.Z. and X.Z.; supervision, X.Z.; project administration, X.Z.; funding acquisition, X.Z. All authors have read and agreed to the published version of the manuscript.

Funding: This work was supported by the National Natural Science Foundation of China (Nos. 22279048, 52066007), Yunnan Major Scientific and Technological Projects (No. 202202AG050017), and the Applied Basic Research Program of Yunnan Province (No. 202101AT070076).

Data Availability Statement: The data presented in this study are available in the article and Supplementary Materials.

Conflicts of Interest: The authors declare no conflict of interest.

References

1. Zhu, X.; Gao, Y.; Wang, X.; Haribal, V.; Liu, J.; Neal, L.M.; Bao, Z.; Wu, Z.; Wang, H.; Li, F. A tailored multi-functional catalyst for ultra-efficient styrene production under a cyclic redox scheme. *Nat. Commun.* **2021**, *12*, 1329. [CrossRef] [PubMed]
2. Sheng, J.; Li, W.-C.; Lu, W.-D.; Yan, B.; Qiu, B.; Gao, X.-Q.; Zhang, R.-P.; Zhou, S.-Z.; Lu, A.-H. Preparation of oxygen reactivity-tuned FeO_x/BN catalyst for selectively oxidative dehydrogenation of ethylbenzene to styrene. *Appl. Catal. B Environ.* **2022**, *305*, 121070. [CrossRef]
3. Mamedova, M.T. Oxidative Dehydrogenation of Ethylbenzene to Styrene on an Exhausted Aluminum Chromium Catalyst. *Russ. J. Appl. Chem.* **2020**, *93*, 488–493. [CrossRef]
4. Xu, J.; Xue, B.; Liu, Y.-M.; Li, Y.-X.; Cao, Y.; Fan, K.-N. Mesostructured Ni-doped ceria as an efficient catalyst for styrene synthesis by oxidative dehydrogenation of ethylbenzene. *Appl. Catal. A Gen.* **2011**, *405*, 142–148. [CrossRef]
5. Balasamy, R.J.; Tope, B.B.; Khurshid, A.; Al-Ali, A.A.S.; Atanda, L.A.; Sagata, K.; Asamoto, M.; Yahiro, H.; Nomura, K.; Sano, T.; et al. Ethylbenzene dehydrogenation over FeO_x/(Mg,Zn)(Al)O catalysts derived from hydrotalcites: Role of MgO as basic sites. *Appl. Catal. A Gen.* **2011**, *398*, 113–122. [CrossRef]
6. Liu, Z.; Sun, X.; Li, Y.; Sui, Z.; Xu, X. A study on the catalytic role of Ce-Co species and coke deposited on ordered mesoporous Al_2O_3 in N_2O-assisted oxidative dehydrogenation of ethylbenzene. *J. Environ. Chem. Eng.* **2022**, *10*, 108609. [CrossRef]
7. Liu, Z.; Li, Y.; Gao, Q.; Sui, Z.; Xu, X. Promotional role of Ceria in N_2O assisted selective oxidative dehydrogenation of ethylbenzene over Ce–Co_2AlO_4 spinel catalysts. *J. Environ. Chem. Eng.* **2021**, *9*, 105512. [CrossRef]
8. Liu, Z.; Li, Y.; Sun, X.; Sui, Z.; Xu, X. Superior performance of K/Co_2AlO_4 catalysts for the oxidative dehydrogenation of ethylbenzene to styrene with N_2O as an oxidant. *J. Ind. Eng. Chem.* **2022**, *112*, 67–75. [CrossRef]
9. Pan, D.; Ru, Y.; Liu, T.; Wang, Y.; Yu, F.; Chen, S.; Yan, X.; Fan, B.; Li, R. Highly efficient and stable ordered mesoporous Ti-Al composite oxide catalyst for oxidative dehydrogenation of ethylbenzene to styrene with CO_2. *Chem. Eng. Sci.* **2022**, *250*, 117388. [CrossRef]
10. Song, K.; Wang, S.; Sun, Q.; Xu, D. Study of oxidative dehydrogenation of ethylbenzene with CO_2 on supported CeO_2-Fe_2O_3 binary oxides. *Arab. J. Chem.* **2020**, *13*, 7357–7369. [CrossRef]
11. Wang, Q.; Li, X.; Li, W.; Feng, J. Promoting effect of Fe in oxidative dehydrogenation of ethylbenzene to styrene with CO_2 (I) preparation and performance of $Ce_{1-x}Fe_xO_2$ catalyst. *Catal. Commun.* **2014**, *50*, 21–24. [CrossRef]
12. Wang, T.; Guan, X.; Lu, H.; Liu, Z.; Ji, M. Nanoflake-assembled Al_2O_3-supported CeO_2-ZrO_2 as an efficient catalyst for oxidative dehydrogenation of ethylbenzene with CO_2. *Appl. Surf. Sci.* **2017**, *398*, 1–8. [CrossRef]
13. Li, X.; Feng, J.; Fan, H.; Wang, Q.; Li, W. The dehydrogenation of ethylbenzene with CO_2 over $Ce_xZr_{1-x}O_2$ solid solutions. *Catal. Commun.* **2015**, *59*, 104–107. [CrossRef]
14. Ji, M.; Zhang, X.; Wang, J.; Park, S.-E. Ethylbenzene dehydrogenation with CO_2 over Fe-doped $MgAl_2O_4$ spinel catalysts: Synergy effect between Fe^{2+} and Fe^{3+}. *J. Mol. Catal. A Chem.* **2013**, *371*, 36–41. [CrossRef]
15. Ch Prathap, V.; Ramana Kumar, V.; Venkata Rao, M.; Nagaiah, P.; Rama Rao, K.S.; David Raju, B. Promotional role of Ceria in CeO_2/$MgAl_2O_4$ spinel catalysts in CO_2 assisted selective oxidative dehydrogenation of ethylbenzene to styrene. *J. Ind. Eng. Chem.* **2019**, *79*, 97–105.
16. Reddy Benjaram, M.; Lee, S.-C.; Han, D.-S.; Park, S.-E. Utilization of carbon dioxide as soft oxidant for oxydehydrogenation of ethylbenzene to styrene over V_2O_5–CeO_2/TiO_2–ZrO_2 catalyst. *Appl. Catal. B Environ.* **2009**, *87*, 230–238. [CrossRef]
17. Jiang, N.; Burri, A.; Park, S.-E. Ethylbenzene to styrene over ZrO_2-based mixed metal oxide catalysts with CO_2 as soft oxidant. *Chin. J. Catal.* **2016**, *37*, 3–15. [CrossRef]
18. Rao, M.V.; Venkateshwarlu, V.; Thirupathaiah, K.; Raju, M.A.; Nagaiah, P.; Mura, K.L.; Raju, B.D.; Rao, K.S.R. Oxidative dehydrogenation of ethylbenzene over γ-Al_2O_3 supported ceria-lanthanum oxide catalysts: Influence of Ce/La composition. *Arab. J. Chem.* **2020**, *13*, 772–782.
19. Wang, T.; Qi, L.; Lu, H.; Ji, M. Flower-like Al_2O_3-supported iron oxides as an efficient catalyst for oxidative dehydrogenation of ethlybenzene with CO_2. *J. CO_2 Util.* **2017**, *17*, 162–169. [CrossRef]

20. Castro Antonio, J.R.; Marques Samuel, P.D.; Soares João, M.; Filho Josue, M.; Saraiva Gilberto, D.; Oliveira Alcineia, C. Nanosized aluminum derived oxides catalysts prepared with different methods for styrene production. *Chem. Eng. J.* **2012**, *209*, 345–355. [CrossRef]
21. Balasamy, R.J.; Khurshid, A.; Al-Ali, A.A.S.; Atanda, L.A.; Sagata, K.; Asamoto, M.; Yahiro, H.; Nomura, K.; Sano, T.; Takehira, K. Ethylbenzene dehydrogenation over binary FeOx–MeOy/Mg(Al)O catalysts derived from hydrotalcites. *Appl. Catal. A Gen.* **2010**, *390*, 225–234. [CrossRef]
22. Rao, K.N.; Reddy, B.M.; Abhishek, B.; Seo, Y.-H.; Jiang, N.; Park, S.-E. Effect of ceria on the structure and catalytic activity of V_2O_5/TiO_2–ZrO_2 for oxidehydrogenation of ethylbenzene to styrene utilizing CO_2 as soft oxidant. *Appl. Catal. B Environ.* **2009**, *91*, 649–656. [CrossRef]
23. Sharma, P.; Dwivedi, R.; Dixit, R.; Batra, M.; Prasad, R. Mechanism evolution for the oxidative dehydrogenation of ethyl benzene to styrene over V_2O_5/TiO_2 catalyst: Computational and kinetic approach. *RSC Adv.* **2015**, *5*, 39635–39642. [CrossRef]
24. Zhou, W.; Lu, W.; Sun, Z.; Qian, J.; He, M.; Chen, Q.; Sun, S. Fe assisted Co-containing hydrotalcites catalyst for the efficient aerobic oxidation of ethylbenzene to acetophenone. *Appl. Catal. A Gen.* **2021**, *624*, 118322. [CrossRef]
25. Zhang, L.; Wu, Z.; Nelson, N.C.; Sadow, A.D.; Slowing, I.I.; Overbury, S.H. Role Of CO_2 As a Soft Oxidant For Dehydrogenation of Ethylbenzene to Styrene over a High-Surface-Area Ceria Catalyst. *ACS Catal.* **2015**, *5*, 6426–6435. [CrossRef]
26. Wang, H.; Cao, F.-X.; Song, Y.-H.; Yang, G.-Q.; Ge, H.-Q.; Liu, Z.-T.; Qu, Y.-Q.; Liu, Z.-W. Two-step hydrothermally synthesized Ce1-xZrxO_2 for oxidative dehydrogenation of ethylbenzene with carbon dioxide. *J. CO_2 Util.* **2019**, *34*, 99–107. [CrossRef]
27. Burri, D.R.; Choi, K.M.; Han, D.-S.; Koo, J.-B.; Park, S.-E. CO_2 utilization as an oxidant in the dehydrogenation of ethylbenzene to styrene over MnO_2-ZrO_2 catalysts. *Catal. Today* **2006**, *115*, 242–247. [CrossRef]
28. Burri, A.; Jiang, N.; Yahyaoui, K.; Park, S.-E. Ethylbenzene to styrene over alkali doped TiO_2-ZrO_2 with CO_2 as soft oxidant. *Appl. Catal. A Gen.* **2015**, *495*, 192–199. [CrossRef]
29. Ansari, M.B.; Park, S.-E. Carbon dioxide utilization as a soft oxidant and promoter in catalysis. *Energy Environ. Sci.* **2012**, *5*, 9419–9437. [CrossRef]
30. Centi, G.; Quadrelli, E.A.; Perathoner, S. Catalysis for CO_2 conversion: A key technology for rapid introduction of renewable energy in the value chain of chemical industries. *Energy Environ. Sci.* **2013**, *6*, 1711–1731. [CrossRef]
31. Mukherjee, D.; Park, S.-E.; Reddy, B.M. CO_2 as a soft oxidant for oxidative dehydrogenation reaction: An eco benign process for industry. *J. CO_2 Util.* **2016**, *16*, 301–312. [CrossRef]
32. Fan, H.-X.; Feng, J.; Li, W.-Y. Promotional effect of oxygen storage capacity on oxy-dehydrogenation of ethylbenzene with CO_2 over κ-$Ce_2Zr_2O_8$(111). *Appl. Surf. Sci.* **2019**, *486*, 411–419. [CrossRef]
33. Xu, J.; Wang, L.-C.; Liu, Y.-M.; Cao, Y.; He, H.-Y.; Fan, K.-N. Mesostructured CeO_2 as an Effective Catalyst for Styrene Synthesis by Oxidative Dehydrogenation of Ethylbenzene. *Catal. Lett.* **2009**, *133*, 307–313. [CrossRef]
34. Gao, Y.; Haeri, F.; He, F.; Li, F. Alkali Metal-Promoted LaxSr2–xFeO4−δ Redox Catalysts for Chemical Looping Oxidative Dehydrogenation of Ethane. *ACS Catal.* **2018**, *8*, 1757–1766. [CrossRef]
35. Li, Y.; Cui, Y.; Zhang, X.; Lu, Y.; Fang, W.; Yang, Y. Optimum ratio of K_2O to CeO_2 in a wet-chemical method prepared catalysts for ethylbenzene dehydrogenation. *Catal. Commun.* **2016**, *73*, 12–15. [CrossRef]
36. da Costa Borges Soares, M.; Barbosa, F.F.; Torres, M.A.M.; Pergher, S.B.C.; Essayem, N.; Braga, T.P. Preferential adsorption of CO_2 on cobalt ferrite sites and its role in oxidative dehydrogenation of ethylbenzene. *Braz. J. Chem. Eng.* **2021**, *38*, 495–510. [CrossRef]
37. Wang, Z.; Qu, Z.; Quan, X.; Wang, H. Selective catalytic oxidation of ammonia to nitrogen over ceria–zirconia mixed oxides. *Appl. Catal. A Gen.* **2012**, *411*, 131–138. [CrossRef]
38. Xu, H.; Sun, M.; Liu, S.; Li, Y.; Wang, J.; Chen, Y. Effect of the calcination temperature of cerium–zirconium mixed oxides on the structure and catalytic performance of $WO_3/CeZrO_2$ monolithic catalyst for selective catalytic reduction of NOx with NH_3. *RSC Adv.* **2017**, *7*, 24177–24187. [CrossRef]
39. Hong, W.-J.; Iwamoto, S.; Inoue, M. Direct NO decomposition over a Ce–Mn mixed oxide modified with alkali and alkaline earth species and CO_2-TPD behavior of the catalysts. *Catal. Today* **2011**, *164*, 489–494. [CrossRef]
40. Miyakoshi, A.; Ueno, A.; Ichikawa, M. XPS and TPD characterization of manganese-substituted iron-potassium oxide catalysts which are selective for dehydrogenation of ethylbenzene into styrene. *Appl. Catal. A-Gen.* **2001**, *219*, 249–258. [CrossRef]
41. Chen, S.; Zeng, L.; Mu, R.; Xiong, C.; Zhao, Z.J.; Zhao, C.; Pei, C.; Peng, L.; Luo, J.; Fan, L.S.; et al. Modulating Lattice Oxygen in Dual-Functional Mo-V-O Mixed Oxides for Chemical Looping Oxidative Dehydrogenation. *J. Am. Chem. Soc.* **2019**, *141*, 18653–18657. [CrossRef] [PubMed]
42. Carrero, C.A.; Schloegl, R.; Wachs, I.E.; Schomaecker, R. Critical Literature Review of the Kinetics for the Oxidative Dehydrogenation of Propane over Well-Defined Supported Vanadium Oxide Catalysts. *ACS Catal.* **2014**, *4*, 3357–3380. [CrossRef]
43. Song, H.; Wang, W.; Sun, J.; Wang, X.; Zhang, X.; Chen, S.; Pei, C.; Zhao, Z.-J. Chemical looping oxidative propane dehydrogenation controlled by oxygen bulk diffusion over $FeVO_4$ oxygen carrier pellets. *Chin. J. Chem. Eng.* **2023**, *53*, 409–420. [CrossRef]

44. Wang, H.; Yang, G.-Q.; Song, Y.-H.; Liu, Z.-T.; Liu, Z.-W. Defect-rich $Ce_{1-x}Zr_xO_2$ solid solutions for oxidative dehydrogenation of ethylbenzene with CO_2. *Catal. Today* **2019**, *324*, 39–48. [CrossRef]
45. Schumacher, L.; Hess, C. The active role of the support in propane ODH over VOx/CeO_2 catalysts studied using multiple operando spectroscopies. *J. Catal.* **2021**, *398*, 29–43. [CrossRef]